Eur. J. Mech. A/Solids 19 (2000) special issue S121–S143

S0997753800001984/FLA

Microplane modelling of cohesive frictional materials

E. Kuhl[1] and E. Ramm[1]

Abstract In the present paper, a constitutive model for cohesive frictional materials will be derived, in which anisotropic elasto–plasticity coupled to anisotropic damage is taken into account. The constitutive formulation is embedded in the framework of microplane theory. Consequently, the basic constitutive laws are characterized on several individual material planes. The homogenized response at one material point can thus be determined from the responses of all these microplanes integrated over the solid angle. Special features of the new microplane formulation will be discussed in comparison to existing microplane models presented in literature. One particular advantage of the microplane formulation presented herein is its close relation to macroscopic invariant–based models which enables the interpretation and identification of the microplane parameters in terms of macroscopically measurable quantities. The appropriate choice of the microplane parameters is illustrated for the model problem of Drucker–Prager elasto–plasticity.

Keywords microplane model, anisotropy, elasto–plasticity coupled to damage, micro–macro relations

1 Introduction

The rapid development of computer technology in the past decades has provoked the development of complex material models which account for material deterioration and plastic effects not only in an isotropic but also in an anisotropic sense. In this context, the microplane model as a natural representative of anisotropic material models has attracted increased attention only recently. It is based on the idea of characterizing the response of a material point through the description of the behavior on various material planes in space. Consequently, complex three dimensional material formulations reduce to easily interpretable two dimensional constitutive laws and the related parameters gain an elementary physical interpretation. Moreover, material anisotropy is incorporated intrinsically through the consideration of individual independent material planes.
Although the basic concept of microplane modelling is more than a hundred years old and originally goes back to MOHR [21], its computational realization in the context of damage of cohesive frictional materials has been developed mainly in the past decade, compare BAŽANT & GAMBAROVA [2], BAŽANT & PRAT [6], CAROL, BAŽANT & PRAT [9] and CAROL, PRAT & BAŽANT [11]. In order to guarantee a unique solution even in the post–critical regime, a non–local version and a gradient–enhanced microplane damage model were presented by BAŽANT & OŽBOLT [4] and KUHL, RAMM & DE BORST [18], respectively. Moreover, a first attempt has been made by CAROL & BAŽANT [8] to apply the basic concept to microplane plasticity as well. Only recently, the microplane model has been embedded into a thermodynamically consistent framework by CAROL, JIRÁSEK

[1] Institute of Mechanics, University of Stuttgart, Pfaffenwaldring 7, D–70550 Stuttgart, Germany.

& BAŽANT [10] and JIRÁSEK [14]. The growing interest in microplane modelling has led to various classes of microplane models each having its own advantages and disadvantages. In this paper, we would like to point out the differences of the individual formulations and suggest a class of models which is closely related to well–known macroscopic constitutive models. Consequently, the formulation can profit from a wide range of experiences made with classical macroscopic material formulations however keeping its freedom to model even more complex constitutive behavior.
This paper is organized as follows. In the second section, the basic equations of a continuous microplane plasticity formulation coupled to microplane damage are derived. Their algorithmic realization based on a spatial and temporal discretization is briefly summarized. Thereby, the underlying class of microplane models is based on three microplane components, namely a normal volumetric, a normal deviatoric and a tangential one. On each microplane, the elastic domain is bounded by a damage loading surface in the microplane strain space and a plastic yield surface in the microplane stress space. In the third section, an alternative class of microplane models based on only two microplane components is discussed. The advantages and disadvantages of the two–component approach in comparison to the three–component model are illustrated in the context of microplane elasticity. In the fourth section, yet another alternative class of microplane models is introduced. In contrast to the basic model, this class is based on the introduction of independent loading functions for each individual microplane component, thus introducing a multiple loading surface formulation on each microplane. A comparison of the plane–wise single surface and the multiple surface formulation is given in the context of microplane damage. Section five deals with a comparison of microplane–based material models with well–known macroscopic invariant–based constitutive formulations. As a result of this comparison, the microplane parameters can easily be related to their macroscopic counterparts. The appropriate choice of the microplane parameters is illustrated for a DRUCKER–PRAGER plasticity formulation. Finally, the microplane–based approach and the classical macroscopic formulation are compared by means of the model problem of a plate with a hole. It should be mentioned, that this article represents the actual state of work and most of the research is still in progress. This is the reason why the final example is restricted to pressure–insensitive metallic materials. However, the extension to pressure–sensitive materials like concrete is planned for the future.

2 Microplane elasto–plasticity coupled to damage

2.1 Continuous formulation

In the present section, a thermodynamically consistent microplane model for elasto–plastically damaging materials will be derived. Its underlying kinematic constraint is based on three microplane components, namely the volumetric, the deviatoric and the tangential microplane strains ϵ_V, ϵ_D and ϵ_T. They can be derived as projections of the overall strain tensor $\boldsymbol{\epsilon}$, which corresponds to the symmetric part of the displacement gradient $\boldsymbol{\epsilon} = \nabla^{sym}\boldsymbol{u}$ in the geometrically linear case. Consequently,

$$\epsilon_V = \boldsymbol{V} : \boldsymbol{\epsilon} \qquad \epsilon_D = \boldsymbol{D} : \boldsymbol{\epsilon} \qquad \epsilon_T = \boldsymbol{T} : \boldsymbol{\epsilon} \tag{1}$$

whereby the individual projection tensors $\boldsymbol{V}$, $\boldsymbol{D}$ and $\boldsymbol{T}$

$$\boldsymbol{V} = \frac{1}{3}\boldsymbol{1} \qquad \boldsymbol{D} = \boldsymbol{n}\otimes\boldsymbol{n} - \frac{1}{3}\boldsymbol{1} \qquad \boldsymbol{T} = \boldsymbol{n}\cdot\boldsymbol{\mathcal{I}}^{sym} - \boldsymbol{n}\otimes\boldsymbol{n}\otimes\boldsymbol{n} \tag{2}$$

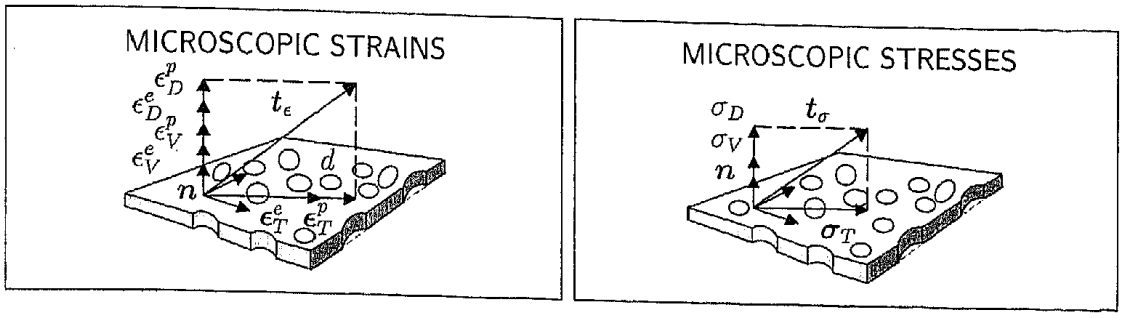

Figure 1: Microplane elasto–plasticity coupled to damage

can be expressed exclusively in terms of the plane's normal $\boldsymbol{n}$, the second order unit tensor $\mathbf{1}$ with the components δ_{ij} and the symmetric part of the fourth order unit tensor $\mathcal{I}^{sym}$ with the components $[\delta_{ik}\,\delta_{jl}+\delta_{il}\,\delta_{jk}]\,/\,2$. When restricting the formulation to a small strain setting, an additive decomposition of the microplane strains into elastic and plastic contributions

$$\epsilon_V = \epsilon_V^e + \epsilon_V^p \qquad \epsilon_D = \epsilon_D^e + \epsilon_D^p \qquad \boldsymbol{\epsilon}_T = \boldsymbol{\epsilon}_T^e + \boldsymbol{\epsilon}_T^p \tag{3}$$

can be assumed. On each microplane, a free energy Ψ^{mic} is introduced as a function of the total strains and a set of internal variables $\boldsymbol{q}$, such that $\Psi^{mic} = \Psi^{mic}(\epsilon_V, \epsilon_D, \boldsymbol{\epsilon}_T, \boldsymbol{q})$. In case of elasto–plasticity coupled to damage, the set of internal variables is composed of the plastic microplane strains as well as a scalar–valued plastic hardening variable κ^p and one common damage variable d for all strain components, $\boldsymbol{q} = [\epsilon_V^p, \epsilon_D^p, \boldsymbol{\epsilon}_T^p, \kappa^p, d]$. The free energy can thus be specified in the following form

$$\Psi^{mic} = [1-d]\Psi^{*mic} \text{ with } \Psi^{*mic} = \frac{1}{2}\left[\epsilon_V^e\,\mathcal{E}_V\,\epsilon_V^e + \epsilon_D^e\,\mathcal{E}_D\,\epsilon_D^e + \boldsymbol{\epsilon}_T^e\cdot\mathcal{E}_T\,\boldsymbol{\epsilon}_T^e\right] + \int_0^{\kappa^p}\phi^p\,d\hat{\kappa}, \tag{4}$$

whereby $\mathcal{E}_V$, $\mathcal{E}_D$ and $\mathcal{E}_T$ denote the volumetric, the deviatoric and the tangential microplane elasticity modulus, respectively. Note, that in general, tangential elasticity would be characterized through a second order tensor $\boldsymbol{\mathcal{E}}_T$. The special choice of $\boldsymbol{\mathcal{E}}_T = \mathcal{E}_T\,\mathbf{1}$ applied herein is based on the assumption of microplane isotropy. Consequently, the three microplane stresses σ_V, σ_D and $\boldsymbol{\sigma}_T$ can be introduced as energetically conjugate quantities to the related strain components

$$\begin{aligned}
\sigma_V &:= \frac{\partial\Psi^{mic}}{\partial\epsilon_V} & \dot{\sigma}_V &= [1-d]\,\mathcal{E}_V\,[\dot{\epsilon}_V - \dot{\epsilon}_V^p]\\
\sigma_D &:= \frac{\partial\Psi^{mic}}{\partial\epsilon_D} & \dot{\sigma}_D &= [1-d]\,\mathcal{E}_D\,[\dot{\epsilon}_D - \dot{\epsilon}_D^p]\\
\boldsymbol{\sigma}_T &:= \frac{\partial\Psi^{mic}}{\partial\boldsymbol{\epsilon}_T} & \dot{\boldsymbol{\sigma}}_T &= [1-d]\,\mathcal{E}_T\,[\dot{\boldsymbol{\epsilon}}_T - \dot{\boldsymbol{\epsilon}}_T^p]
\end{aligned} \tag{5}$$

while the yield stress ϕ^p is introduced as conjugate quantity to the plastic hardening variable κ^p

$$\phi^p := -\frac{\partial\Psi^{mic}}{\partial\kappa^p} \qquad \dot{\phi}^p = H^p\,\dot{\kappa}^p, \tag{6}$$

whereby H^p denotes the plastic hardening modulus. The undamaged energy Ψ^{*mic} denoted by Y can be understood as conjugate quantity to the damage variable

$$Y := -\frac{\partial\Psi^{mic}}{\partial d} = \Psi^{*mic}. \tag{7}$$

Moreover, the scalar product of the partial derivative of the free energy with respect to the set of internal variables with the evolution of the internal variables themselves is introduced as microscopic dissipation $\mathcal{D}^{mic}$ with

$$\mathcal{D}^{mic} := -\frac{\partial \Psi^{mic}}{\partial \boldsymbol{q}} \star \dot{\boldsymbol{q}} = Y\,\dot{d} + \sigma_V\,\dot{\epsilon}_V^p + \sigma_D\,\dot{\epsilon}_D^p + \boldsymbol{\sigma}_T \cdot \dot{\boldsymbol{\epsilon}}_T^p - \phi^p \dot{\kappa}^p. \tag{8}$$

The process of damage evolution is governed by a damage loading function Φ^d which is introduced as the difference of a function ϕ^d of the damage driving force Y and the damage variable d as a function of a history parameter κ^d.

$$\Phi^d = \phi^d(Y) - d(\kappa^d) \tag{9}$$

In this case, Φ^d is defined in an energy–based fashion according to SIMO & JU [23], but of course alternative strain– and stress–based formulations could be thought of as well. Note, however, that stress–based formulations seem to be physically inadequate when plastic effects are incorporated as stated by JU [15]. The classical KUHN–TUCKER conditions and the consistency condition take the following form

$$\Phi^d \leq 0 \qquad \dot{\gamma}^d \geq 0 \qquad \Phi^d\,\dot{\gamma}^d = 0 \qquad \dot{\Phi}^d\,\dot{\gamma}^d = 0, \tag{10}$$

whereby $\dot{\gamma}^d$ denotes a damage multiplier. The evaluation of the consistency condition yields the equivalence of this damage multiplier and the rate of the damage driving force Y, such that $\dot{Y} = \dot{\gamma}^d$. In case of a monotonic function ϕ^d, the calculation of the damage variable thus reduces to the following simple format

$$d = \phi^d(\kappa^d) \qquad \text{with} \qquad \kappa^d = \max_{-\infty<t<\tau}(Y(t), \kappa_0^d) \qquad \text{and} \qquad H^d := \frac{\partial \phi^d}{\partial \kappa^d}, \tag{11}$$

with κ_0^d denoting a damage threshold value. From a physical point of view, the material is damaged through the formation of microcracks and microvoids. Thus, the effective stresses in the remaining material are higher than the nominal stresses and plastic yielding will start remarkably earlier than in the undamaged material. Accordingly, microplane plasticity is formulated in the effective stress space, whereby the effective microplane stresses can be understood as the nominal stresses weighted by the undamaged area fraction $[1-d]$ such that

$$\bar{\sigma}_V := \frac{\sigma_V}{1-d} \qquad \bar{\sigma}_D := \frac{\sigma_D}{1-d} \qquad \bar{\boldsymbol{\sigma}}_T := \frac{\boldsymbol{\sigma}_T}{1-d}. \tag{12}$$

Plastic yielding on the microplane is governed by a yield function Φ^p, which is introduced as the difference of an equivalent stress φ^p and the yield stress ϕ^p

$$\Phi^p = \varphi^p(\bar{\sigma}_V, \bar{\sigma}_D, \bar{\boldsymbol{\sigma}}_T) - \phi^p(\kappa^p). \tag{13}$$

In the following, the normals to the yield surface Φ^d in the effective stress space will be denoted by $\bar{\nu}_V$, $\bar{\nu}_D$ and $\bar{\boldsymbol{\nu}}_T$

$$\bar{\nu}_V := \frac{\partial \Phi^p}{\partial \bar{\sigma}_V} \qquad \bar{\nu}_D := \frac{\partial \Phi^p}{\partial \bar{\sigma}_D} \qquad \bar{\boldsymbol{\nu}}_T := \frac{\partial \Phi^p}{\partial \bar{\boldsymbol{\sigma}}_T}. \tag{14}$$

In a general non–associated plasticity formulation, these normals can be different from the directions of plastic flow $\bar{\mu}_V$, $\bar{\mu}_D$ and $\bar{\boldsymbol{\mu}}_T$ which can be understood as normals to a plastic potential Φ^{*p} with

$$\bar{\mu}_V := \frac{\partial \Phi^{*p}}{\partial \bar{\sigma}_V} \qquad \bar{\mu}_D := \frac{\partial \Phi^{*p}}{\partial \bar{\sigma}_D} \qquad \bar{\boldsymbol{\mu}}_T := \frac{\partial \Phi^{*p}}{\partial \bar{\boldsymbol{\sigma}}_T}. \tag{15}$$

The plastic flow rules and the evolution of the plastic hardening parameter κ^p can thus be expressed in terms of these flow directions and the plastic multiplier $\dot{\gamma}^p$

$$\dot{\epsilon}_V^p = \dot{\gamma}^p \, \bar{\mu}_V \qquad \dot{\epsilon}_D^p = \dot{\gamma}^p \, \bar{\mu}_D \qquad \dot{\boldsymbol{\epsilon}}_T^p = \dot{\gamma}^p \, \bar{\boldsymbol{\mu}}_T \qquad \dot{\kappa}^p = \dot{\gamma}^p. \tag{16}$$

The related KUHN–TUCKER conditions and the consistency condition

$$\Phi^p \leq 0 \qquad \dot{\gamma}^p \geq 0 \qquad \Phi^p \, \dot{\gamma}^p = 0 \qquad \dot{\Phi}^p \, \dot{\gamma}^p = 0 \tag{17}$$

govern the loading–unloading process, whereby the latter defines the plastic multiplier $\dot{\gamma}^p$

$$\dot{\gamma}^p = \frac{1}{h^p} \left[\bar{\nu}_V \, \mathcal{E}_V \, \boldsymbol{V} + \bar{\nu}_D \, \mathcal{E}_D \, \boldsymbol{D} + \bar{\boldsymbol{\nu}}_T \cdot \mathcal{E}_T \cdot \boldsymbol{T} \right] : \dot{\boldsymbol{\epsilon}}, \tag{18}$$

with $h^p := \bar{\nu}_V \, \mathcal{E}_V \, \bar{\mu}_V + \bar{\nu}_D \, \mathcal{E}_D \, \bar{\mu}_D + \bar{\boldsymbol{\nu}}_T \cdot \mathcal{E}_T \cdot \bar{\boldsymbol{\mu}}_T + H^p$. The macroscopic response can be determined by making use of the following fundamental assumption according to CAROL, JIRÁSEK & BAŽANT [10]

$$\Psi^{mac} = \frac{3}{4\pi} \int_\Omega \Psi^{mic} d\Omega, \tag{19}$$

which relates the macroscopic free energy Ψ^{mac} to the integral of all microplane energies Ψ^{mic} over the solid angle Ω. Consequently, the overall stress tensor $\boldsymbol{\sigma}$ can be derived by evaluating the second principle of thermodynamics in form of the CLAUSIUS–DUHEM inequality as $\boldsymbol{\sigma} := \partial \Psi^{mac} / \partial \boldsymbol{\epsilon}$. With the help of the definition of the microscopic stresses (5), the evolution of the macroscopic stresses can be written as

$$\dot{\boldsymbol{\sigma}} = \frac{3}{4\pi} \int_\Omega [1-d] \left[\boldsymbol{V} \, \mathcal{E}_V \, [\dot{\epsilon}_V - \dot{\epsilon}_V^p] + \boldsymbol{D} \, \mathcal{E}_D \, [\dot{\epsilon}_D - \dot{\epsilon}_D^p] + \boldsymbol{T}^T \cdot \mathcal{E}_T \, [\dot{\boldsymbol{\epsilon}}_T - \dot{\boldsymbol{\epsilon}}_T^p] \right] d\Omega. \tag{20}$$

Moreover, the macroscopic dissipation

$$\mathcal{D}^{mac} = \frac{3}{4\pi} \int_\Omega \mathcal{D}^{mic} \, d\Omega \geq 0 \tag{21}$$

and the overall tangent operator of microplane elasto-plasticity coupled to damage $\mathcal{E}_{tan}^{dp} := \mathrm{d}\boldsymbol{\sigma} \, / \, \mathrm{d}\boldsymbol{\epsilon}$ can be expressed as follows

$$\begin{aligned}
\mathcal{E}_{tan}^{dp} = & \frac{3}{4\pi} \int_\Omega [1-d] \qquad [\mathcal{E}_V \boldsymbol{V} \otimes \boldsymbol{V} + \mathcal{E}_D \boldsymbol{D} \otimes \boldsymbol{D} + \mathcal{E}_T \boldsymbol{T}^T \cdot \boldsymbol{T}] \qquad d\Omega \\
& - \frac{3}{4\pi} \int_\Omega \frac{1-d}{h^p} [\boldsymbol{V} \mathcal{E}_V \bar{\mu}_V + \boldsymbol{D} \mathcal{E}_D \bar{\mu}_D + \boldsymbol{T}^T \cdot \mathcal{E}_T \bar{\boldsymbol{\mu}}_T] \otimes [\bar{\nu}_V \mathcal{E}_V \boldsymbol{V} + \bar{\nu}_D \mathcal{E}_D \boldsymbol{D} + \bar{\boldsymbol{\nu}}_T \cdot \mathcal{E}_T \boldsymbol{T}] d\Omega \\
& - \frac{3}{4\pi} \int_\Omega H^d \qquad [\boldsymbol{V} \bar{\sigma}_V + \boldsymbol{D} \bar{\sigma}_D + \boldsymbol{T}^T \cdot \bar{\boldsymbol{\sigma}}_T] \otimes [\bar{\sigma}_V \boldsymbol{V} + \bar{\sigma}_D \boldsymbol{D} + \bar{\boldsymbol{\sigma}}_T \cdot \boldsymbol{T}] \qquad d\Omega \\
& + \frac{3}{4\pi} \int_\Omega \frac{H^d \phi^{*p}}{h^p} \qquad [\boldsymbol{V} \bar{\sigma}_V + \boldsymbol{D} \bar{\sigma}_D + \boldsymbol{T}^T \cdot \bar{\boldsymbol{\sigma}}_T] \otimes [\bar{\nu}_V \mathcal{E}_V \boldsymbol{V} + \bar{\nu}_D \mathcal{E}_D \boldsymbol{D} + \bar{\boldsymbol{\nu}}_T \cdot \mathcal{E}_T \boldsymbol{T}] d\Omega,
\end{aligned} \tag{22}$$

whereby $\phi^{*p} := \bar{\sigma}_V \, \bar{\mu}_V + \bar{\sigma}_D \, \bar{\mu}_D + \bar{\boldsymbol{\sigma}}_T \cdot \bar{\boldsymbol{\mu}}_T + \phi^p$. Note that the first row of equation (22) represents the elastic material operator multiplied by $[1-d]$. The combination of the first and the second row characterizes the elasto-plastic tangent operator, again multiplied by $[1-d]$, while the combination of the first and third row denotes the tangent operator of microplane–based elasto–damage. The last row takes into account the contributions due to plastic–damage coupling.

2.2 Algorithmic formulation

In the continuous formulation described in the previous section, the homogenization procedure is based on an integration over the solid angle Ω. In the computational algorithm, however, this integration is performed numerically by replacing each integral expression by a discrete sum as $\int_\Omega (\bullet)\, d\Omega \approx \sum_{I=1}^{n_{mp}} (\bullet)^I\, w^I$. The related integrants $(\bullet)^I$ are thus evaluated at $I = 1, .., n_{mp}$ discrete integration points and weighted by the corresponding weighting coefficients w^I. In the context of the microplane model, each of these integration points corresponds to one discrete microplane.

In addition to the spatial discretization of the solid angle, a temporal discretization has to be performed by dividing the time interval of interest into $n = 1, .., n_{step}$ discrete time steps. The computational solution procedure for the rate equations of elasto-plastic damaging materials is embedded in a three–step operator split algorithm. This algorithm, which is composed of an elastic predictor and a plastic and damage corrector step, has originally been proposed by JU [15] for isotropic elasto–plastic damaging materials. As the spatial interaction of the individual microplanes has been assumed to be negligibly small, this three–step operator split algorithm can be applied on the microplane level independently for each microplane.

Therefore, it is assumed, that at the beginning of each time step t^n, the values of the internal variables ϵ_V^{pn}, ϵ_D^{pn}, ϵ_T^{pn}, κ^{pn} and κ^{dn} of each microplane as well as the overall strain and stress tensor $\boldsymbol{\epsilon}^n$ and $\boldsymbol{\sigma}^n$ are known. Moreover, the incremental displacement field $\Delta \boldsymbol{u}$ and accordingly, the update of the strain tensor $\boldsymbol{\epsilon}^{n+1} = \boldsymbol{\epsilon}^n + \Delta\boldsymbol{\epsilon}$ with $\Delta\boldsymbol{\epsilon} = \Delta\nabla^{sym}\boldsymbol{u}$ are assumed to be given. In the first step of the algorithm, an elastic trial state is calculated, for which the strain increment $\Delta\boldsymbol{\epsilon}$ is assumed to be completely elastic and

$$\epsilon_V^{e\,trial} = \boldsymbol{V} : \boldsymbol{\epsilon} - \epsilon_V^{pn} \qquad \epsilon_D^{e\,trial} = \boldsymbol{D} : \boldsymbol{\epsilon} - \epsilon_D^{pn} \qquad \boldsymbol{\epsilon}_T^{e\,trial} = \boldsymbol{T} : \boldsymbol{\epsilon} - \boldsymbol{\epsilon}_T^{pn}. \tag{23}$$

Consequently, the related values of the plastic strains

$$\epsilon_V^{p\,trial} = \epsilon_V^{pn} \qquad \epsilon_D^{p\,trial} = \epsilon_D^{pn} \qquad \boldsymbol{\epsilon}_T^{p\,trial} = \boldsymbol{\epsilon}_T^{pn} \tag{24}$$

and the internal variables $\kappa^{p\,trial}$ and $\kappa^{d\,trial}$

$$\kappa^{p\,trial} = \kappa^{pn} \qquad \text{and} \qquad \kappa^{d\,trial} = \kappa^{dn} \tag{25}$$

are identical to their values of the beginning of the time step and $d^{trial} = \phi^d(\kappa^{d\,trial})$. The resulting trial stresses

$$\sigma_V^{trial} = [1 - d^{trial}]\mathcal{E}_V \epsilon_V^{e\,trial} \qquad \sigma_D^{trial} = [1 - d^{trial}]\mathcal{E}_D \epsilon_D^{e\,trial} \qquad \boldsymbol{\sigma}_T^{trial} = [1 - d^{trial}]\mathcal{E}_T \boldsymbol{\epsilon}_T^{e\,trial} \tag{26}$$

and the effective trial stresses can thus be expressed as follows

$$\bar{\sigma}_V^{trial} = \frac{\sigma_V^{trial}}{1 - d^{trial}} \qquad \bar{\sigma}_D^{trial} = \frac{\sigma_D^{trial}}{1 - d^{trial}} \qquad \bar{\boldsymbol{\sigma}}_T^{trial} = \frac{\boldsymbol{\sigma}_T^{trial}}{1 - d^{trial}}. \tag{27}$$

In the second step, the plastic yield function

$$\Phi^{p\,trial} = \varphi^p(\bar{\sigma}_V^{trial}, \bar{\sigma}_D^{trial}, \bar{\boldsymbol{\sigma}}_T^{trial}) - \phi^p(\kappa^{p\,trial}) \tag{28}$$

is evaluated on the basis of the elastic trial values. If $\Phi^{p\,trial} \leq 0$, the current step is non–plastic and consequently, the plastic variables at the end of the time step are identical to their trial values and $(\bullet)^{p\,n+1} = (\bullet)^{p\,trial}$. However, if $\Phi^{p\,trial} > 0$, the KUHN–TUCKER

conditions are violated and a plastic corrector step has to be performed to return the trial state back to the yield surface. The plastic corrector is based on the calculation of the incremental plastic multiplier $\Delta\gamma^p$ which determines the update of the plastic strains

$$\epsilon_V^{p\,n+1} = \epsilon_V^{p\,trial} + \Delta\gamma^p \frac{\partial \Phi^{*p}}{\partial \bar{\sigma}_V^{n+1}} \quad \epsilon_D^{p\,n+1} = \epsilon_D^{p\,trial} + \Delta\gamma^p \frac{\partial \Phi^{*p}}{\partial \bar{\sigma}_D^{n+1}} \quad \epsilon_T^{p\,n+1} = \epsilon_T^{p\,trial} + \Delta\gamma^p \frac{\partial \Phi^{*p}}{\partial \bar{\boldsymbol{\sigma}}_T^{n+1}}, \tag{29}$$

the hardening variable

$$\kappa^{p\,n+1} = \kappa^{p\,trial} + \Delta\gamma^p \tag{30}$$

and the effective stress state

$$\bar{\sigma}_V^{n+1} = \bar{\sigma}_V^{trial} - \mathcal{E}_V \Delta\gamma^p \frac{\partial \Phi^{*p}}{\partial \bar{\sigma}_V^{n+1}} \quad \bar{\sigma}_D^{n+1} = \bar{\sigma}_D^{trial} - \mathcal{E}_D \Delta\gamma^p \frac{\partial \Phi^{*p}}{\partial \bar{\sigma}_D^{n+1}} \quad \bar{\boldsymbol{\sigma}}_T^{n+1} = \bar{\boldsymbol{\sigma}}_T^{trial} - \mathcal{E}_T \Delta\gamma^p \frac{\partial \Phi^{*p}}{\partial \bar{\boldsymbol{\sigma}}_T^{n+1}}. \tag{31}$$

With the help of these variables, the current energy release rate

$$Y^{n+1} = \frac{1}{2}\left[\epsilon_V^{e\,n+1} \mathcal{E}_V \epsilon_V^{e\,n+1} + \epsilon_D^{e\,n+1} \mathcal{E}_D \epsilon_D^{e\,n+1} + \boldsymbol{\epsilon}_T^{e\,n+1} \cdot \mathcal{E}_T \boldsymbol{\epsilon}_T^{e\,n+1}\right] + \int_0^{\kappa^p} \phi^p \, d\hat{\kappa}^{p\,n+1}. \tag{32}$$

can be calculated as driving force for the evolution of damage. Finally, the third step can be performed based on the evaluation of the damage loading function

$$\Phi^{d\,trial} = \phi^d(Y^{d\,n+1}) - d(\kappa^{d\,trial}). \tag{33}$$

If $\Phi^{d\,trial} \leq 0$, the current step is non–damaging and the damage variables are identical to their trial values as $(\bullet)^{d\,n+1} = (\bullet)^{d\,trial}$. If $\Phi^{d\,trial} < 0$, a damage corrector step has to be performed to return the trial state back to the damage loading surface. In this case, the update of the damage variable can be calculated explicitly as

$$d^{n+1} = \phi(\kappa^{d\,n+1}) \qquad \text{with} \qquad \kappa^{d\,n+1} = \max_{-\infty < t < \tau} (Y^{n+1}, \kappa_0^d). \tag{34}$$

Accordingly, the nominal stresses at the end of the time step can be calculated as follows

$$\sigma_V^{n+1} = [1 - d^{n+1}]\bar{\sigma}_V^{n+1} \qquad \sigma_D^{n+1} = [1 - d^{n+1}]\bar{\sigma}_D^{n+1} \qquad \boldsymbol{\sigma}_T^{n+1} = [1 - d^{n+1}]\bar{\boldsymbol{\sigma}}_T^{n+1}. \tag{35}$$

Note, that although plasticity and damage are coupled in the continuous rate equations of section 2.1, the operator split renders a fully decoupled elasto–plastic damage algorithm. Finally, the overall stress tensor can be calculated as the sum over all $I = 1, .., n_{mp}$ discrete microplane stresses weighted by their individual projection tensors $\boldsymbol{V}^I$, $\boldsymbol{D}^I$ and $\boldsymbol{T}^I$ and multiplied by the corresponding weighting coefficients w^I as

$$\boldsymbol{\sigma}^{n+1} = \sum_{I=1}^{n_{mp}} \left[\boldsymbol{V}^I \sigma_V^{I\,n+1} + \boldsymbol{D}^I \sigma_D^{I\,n+1} + \boldsymbol{T}^{IT} \cdot \boldsymbol{\sigma}_T^{I\,n+1}\right] w^I. \tag{36}$$

2.3 Model problem - Uniaxial tension

The basic features of the proposed model of microplane elasto–plasticity coupled to damage will now be elaborated with the help of an academic model problem. Therefore, the homogeneous response of a single 1 mm^3 large eight–noded finite element is analyzed under uniaxial tension. The elastic parameters are chosen as E=30000 N/mm^2 and $\nu = 0.2$. With the assumption of $\mathcal{E}_D = 0$ N/mm^2, the remaining microplane elasticity parameters take the values $\mathcal{E}_V = 50000$ N/mm^2 and $\mathcal{E}_T = 41666.67$ N/mm^2. The

evolution of damage is governed by the damage loading function, $\Phi^d = \phi^d - d$ with $\phi^d = 1 - \kappa_0^d/\kappa^d[1 - \alpha^d + \alpha^d \exp[\beta^d[\kappa_0^d - \kappa^d]]]$ defining an exponential damage growth. The related damage threshold value $\kappa_0^d = 0.0005$ N/mm^2, the ratio of maximum damage $\alpha^d = 0.90$ and the parameter $\beta^d = 100$ [N/mm^2]$^{-1}$ take the given values. Moreover, the plastic yield function $\Phi^p = \varphi^p - \phi^p$ is defined through the following equivalent stress of DRUCKER–PRAGER type $\varphi^p = ||\boldsymbol{\sigma}_T|| + \alpha^p \sigma_V$ and the yield stress $\phi^p = \sigma_Y^p + H^p \kappa^p$. Thereby, the initial yield stress $\sigma_Y^p = 15$ N/mm^2 and the hardening parameter $H^p = 10$ N/mm^2 define a linear hardening behavior. The friction coefficient α^p is chosen as $\alpha^p = 1.0$ to introduce a volumetric deviatoric coupling on the microplane level. An associated flow rule with $\Phi^{*p} \equiv \Phi^p$ is assumed.

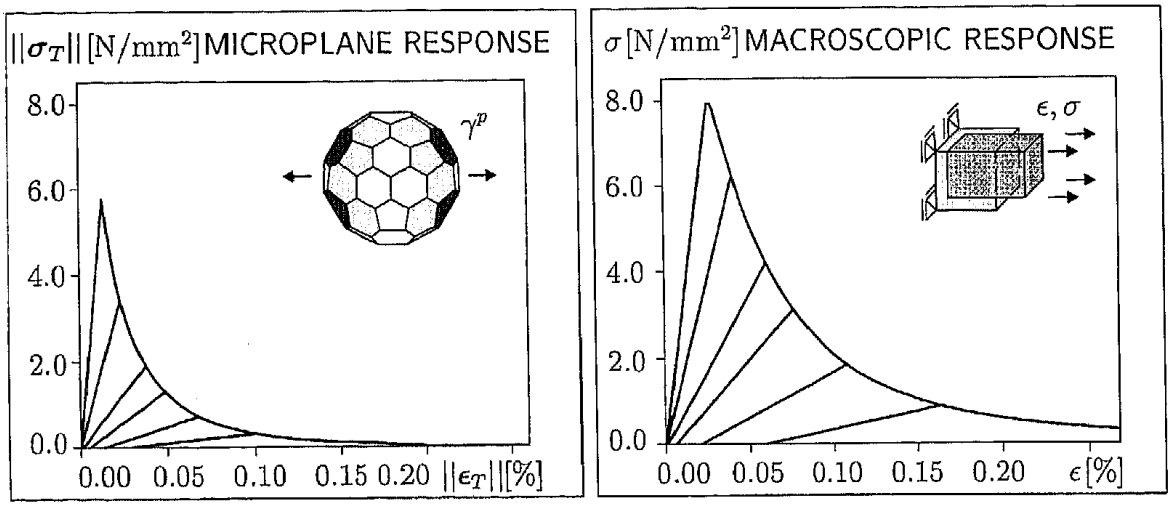

Figure 2: Microscopic and macroscopic response – Uniaxial tension

Figure 2, left, shows the response on the microplane level which is defined through the choice of microplane laws and parameters. For the sake of transparency, only the tangential stress strain behavior of one particular microplane is illustrated. The related volumetric stress strain curve shows a similar behavior with a peak stress of about 2.0 N/mm^2. Obviously, for the given set of parameters, in first stage, the inelastic response is dominated by damage only. The first unloading branch returns straight to the origin without showing any irreversible strains. Under further loading, however, the inelastic material behavior is clearly governed by a combination of damage and plasticity. Consequently, during the following unloading cycles, stiffness degradation as well as inelastic strains can be observed. The highly anisotropic distribution of the plastic multiplier γ^p is sketched in the small figure inside the diagram. The amount of plastic straining apparently takes maximum values under approximately 45^0 towards the loading direction. Figure 2, right, documents the macroscopic response on the material point level as a result of the spatial integration of all microplane responses. The macroscopic stress component in the loading direction is plotted versus the related strain component. Note, that the macroscopic peak stress is remarkably higher, than the tangential peak stress on the microplane level. This difference is obviously caused by the volumetric stresses which also contribute to the macroscopic response. Nevertheless, the shape of the overall stress strain curve is similar to the response on the microplane level. Again, the onset of damage takes place before plastic effects can be observed. In a later stage, the overall response is governed by a combination of damage and plasticity, as expected.

3 Microplane elasticity: Choice of relevant microplane components

In this section, the constitutive equations presented in the previous section will be restricted to microplane elasticity, for which no internal variables are needed. Consequently, the microscopic and the macroscopic dissipation vanish identically with $\mathcal{D}^{mic} \equiv 0$ and thus $\mathcal{D}^{mac} \equiv 0$. While in the first part of this section, a volumetric–deviatoric–tangential model will be presented which can be considered as a special case of the basic model introduced in section 2.1 the second part will be dedicated to an alternative microplane formulation, for which the volumetric and the deviatoric component have been summarized in only one normal component ϵ_N with $\epsilon_N = \epsilon_V + \epsilon_D$. The second model thus represents the most natural choice of microplane variables based on only two components. Finally, the volumetric–deviatoric–tangential model and the normal–tangential model will be compared and discussed by means of their features and ranges of application.

3.1 Volumetric–deviatoric–tangential model

As indicated in figure 3 and used already in section 2, the first microplane elasticity formulation will be based on three microplane strain components, namely a scalar–valued

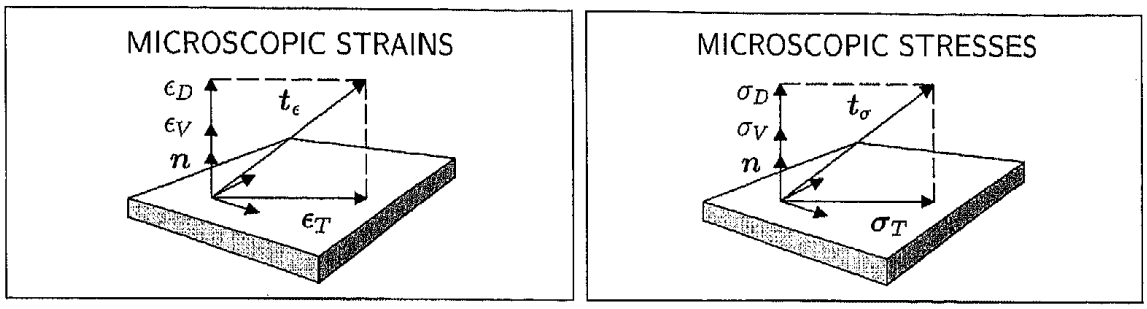

Figure 3: Model with volumetric, deviatoric and tangential microplane components

volumetric and deviatoric strain component associated with the direction normal to the plane and a tangential strain vector lying in the plane of consideration

$$\epsilon_V = \boldsymbol{V} : \boldsymbol{\epsilon} \qquad \epsilon_D = \boldsymbol{D} : \boldsymbol{\epsilon} \qquad \boldsymbol{\epsilon}_T = \boldsymbol{T} : \boldsymbol{\epsilon}. \tag{37}$$

Consequently, the strain vector of the related plane can be expressed as $\boldsymbol{t}_\epsilon = [\ \epsilon_V + \epsilon_D\ ]\,\boldsymbol{n} + \boldsymbol{\epsilon}_T$. The volumetric, deviatoric and tangential projection tensor are given as follows

$$\boldsymbol{V} = \frac{1}{3}\,\mathbf{1} \qquad \boldsymbol{D} = \boldsymbol{n} \otimes \boldsymbol{n} - \frac{1}{3}\,\mathbf{1} \qquad \boldsymbol{T} = \boldsymbol{n} \cdot \boldsymbol{\mathcal{I}}^{sym} - \boldsymbol{n} \otimes \boldsymbol{n} \otimes \boldsymbol{n}, \tag{38}$$

whereby their fourth order products show the following integration properties when integrated analytically over the solid angle Ω, compare LUBARDA & KRAJCINOVIC [20] and KANATANI [16]

$$\begin{aligned} \tfrac{3}{4\pi}\textstyle\int_\Omega \ \boldsymbol{V} \otimes \boldsymbol{V} \ d\Omega &= \boldsymbol{\mathcal{I}}^{vol} \\ \tfrac{3}{4\pi}\textstyle\int_\Omega \ \boldsymbol{D} \otimes \boldsymbol{D} \ d\Omega &= \tfrac{2}{5}\,\boldsymbol{\mathcal{I}}^{dev} \\ \tfrac{3}{4\pi}\textstyle\int_\Omega \ \boldsymbol{T}^T \cdot \boldsymbol{T} \ d\Omega &= \tfrac{3}{5}\,\boldsymbol{\mathcal{I}}^{dev} \ . \end{aligned} \tag{39}$$

Herein, $\mathcal{I}^{vol} = \mathbf{1} \otimes \mathbf{1}$ denotes the volumetric part of the fourth order unit tensor, while $\mathcal{I}^{dev} = \mathcal{I} - \mathcal{I}^{vol}$ denotes its deviatoric part. A purely elastic material behavior can be characterized exclusively in terms of the microplane strains, such that the free energy of each microplane can be specified as follows,

$$\Psi^{mic} = \frac{1}{2}\, \epsilon_V\, \mathcal{E}_V\, \epsilon_V + \frac{1}{2}\, \epsilon_D\, \mathcal{E}_D\, \epsilon_D + \frac{1}{2}\, \boldsymbol{\epsilon}_T \cdot \boldsymbol{\mathcal{E}}_T\, \boldsymbol{\epsilon}_T. \tag{40}$$

whereby $\mathcal{E}_V$, $\mathcal{E}_D$ and $\mathcal{E}_T$ denote the volumetric, the deviatoric and the tangential elasticity modulus, respectively. The free energy defines the microplane stresses as energetically conjugate quantities to the microplane strains as

$$\sigma_V := \mathcal{E}_V\, \epsilon_V \qquad \sigma_D := \mathcal{E}_D\, \epsilon_D \qquad \boldsymbol{\sigma}_T := \boldsymbol{\mathcal{E}}_T \cdot \boldsymbol{\epsilon}_T, \tag{41}$$

and the related stress vector $\boldsymbol{t}_\sigma$ results as $\boldsymbol{t}_\sigma = [\sigma_V + \sigma_D]\, \boldsymbol{n} + \boldsymbol{\sigma}_T$. The general definition of the macroscopic stress tensor (20) thus reduces to

$$\boldsymbol{\sigma} = \frac{3}{4\pi} \int_\Omega \boldsymbol{V}\, \mathcal{E}_V\, \epsilon_V + \boldsymbol{D}\, \mathcal{E}_D\, \epsilon_D + \boldsymbol{T}^T \cdot \boldsymbol{\mathcal{E}}_T\, \boldsymbol{\epsilon}_T\, d\Omega, \tag{42}$$

while the overall tangent moduli of equation (22) reduce to the following expression for the elastic moduli

$$\boldsymbol{\mathcal{E}} = \frac{3}{4\pi} \int_\Omega \mathcal{E}_V\, \boldsymbol{V} \otimes \boldsymbol{V} + \mathcal{E}_D\, \boldsymbol{D} \otimes \boldsymbol{D} + \boldsymbol{\mathcal{E}}_T\, \boldsymbol{T}^T \cdot \boldsymbol{T}\, d\Omega. \tag{43}$$

By assuming an isotropic distribution of the elastic constants $\mathcal{E}_V$, $\mathcal{E}_D$ and $\boldsymbol{\mathcal{E}}_T$ and making use of the integration formulae (39), the above equation can be evaluated analytically and compared with the elasticity tensor of HOOKE's law. This comparison results in the following relations between the elastic microplane moduli $\mathcal{E}_V$, $\mathcal{E}_D$ and $\boldsymbol{\mathcal{E}}_T$ and the macroscopic elastic bulk and shear modulus K and G with

$$\mathcal{E}_V = 3\, K \qquad \text{and} \qquad \mathcal{E}_D + \boldsymbol{\mathcal{E}}_T = \frac{10}{3}\, G. \tag{44}$$

Remarks on the volumetric-deviatoric-tangential models

- The determination of three elastic microplane moduli $\mathcal{E}_V$, $\mathcal{E}_D$ and $\boldsymbol{\mathcal{E}}_T$ in terms of only two elastic constants, for example K and G, is non–unique. Equation (44) documents, that either $\mathcal{E}_D$ or $\boldsymbol{\mathcal{E}}_T$ can be chosen independently. However, in any case, the volumetric modulus has to be related to the bulk modulus while both deviatoric moduli can be expressed exclusively in terms of the shear modulus. This is what one intuitively expects.
- An advantage of this class of models is, that the whole range of POISSON's ratio $-1 \leq \nu \leq 0.5$ can be covered with positive microplane moduli $\mathcal{E}_V \geq 0$, $\mathcal{E}_D \geq 0$ and $\boldsymbol{\mathcal{E}}_T \geq 0$, as discussed in detail by CAROL & BAŽANT [8].
- In the volumetric–deviatoric–tangential model, the individual stress and strain components ϵ_V and σ_V, ϵ_D and σ_D, $\boldsymbol{\epsilon}_T$ and $\boldsymbol{\sigma}_T$ have been introduced as energetically conjugate pairs through equation (41). Consequently, the volumetric and the deviatoric behavior can be controlled independently. However, in general it is not possible, to characterize the overall stress tensor $\boldsymbol{\sigma}$ in terms of the stress vectors $\boldsymbol{t}_\sigma$, and $\boldsymbol{\sigma} \neq \frac{3}{4\pi} \int_\Omega [\boldsymbol{t}_\sigma \otimes \boldsymbol{n}]^{sym} d\Omega$.

- Note, that the original microplane model of BAŽANT & PRAT [6] is based on an alternative homogenization procedure. It induces an artificial coupling of the normal volumetric and the normal deviatoric component, since the overall stress tensor is introduced as $\boldsymbol{\sigma} = \frac{3}{4\pi}\int_\Omega [\boldsymbol{t}_\sigma \otimes \boldsymbol{n}]^{sym} d\Omega$. However, their formulation, which does not include any work conjugate pairs of microplane strains and stresses, is thermodynamically inconsistent and may result in non-symmetric material operators.
- The microplane model of FICHANT, LA BORDERIE & PIJAUDIER-CABOT [12] which takes into account different damage laws for the volumetric and the deviatoric behavior, can be understood as a special case of this class of models by setting $\mathcal{E}_D \equiv 0$. Moreover, with the assumption of $\mathcal{E}_D \equiv 0$, specific representatives of this class of models can be related to macroscopic constitutive formulations based on invariant representations as shown by KUHL, RAMM & WILLAM [19].

3.2 Normal–tangential models

In this section, we will discuss the most natural type of microplane formulation which is based on only two microplane components, namely a scalar–valued quantity ϵ_N and a tangential vector $\boldsymbol{\epsilon}_T$, as illustrated in figure 4. Note, that the normal strain component

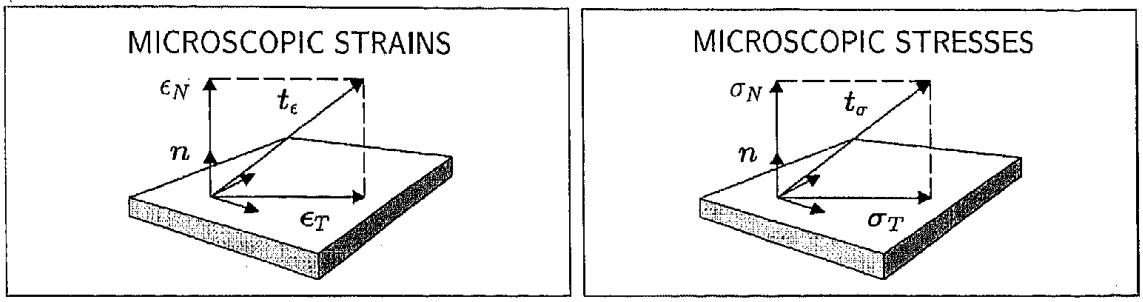

Figure 4: Model with normal and tangential microplane components

can be understood as the sum of the volumetric and the deviatoric strains introduced in equation (37), such that $\epsilon_N = \epsilon_V + \epsilon_D$. In case of a kinematically constraint microplane formulation, the normal and the tangential strain component can be determined as normal and tangential projections of the strain vector $\boldsymbol{t}_\epsilon = \boldsymbol{\epsilon} \cdot \boldsymbol{n}$ with

$$\epsilon_N = \boldsymbol{N} : \boldsymbol{\epsilon} \qquad \boldsymbol{\epsilon}_T = \boldsymbol{T} : \boldsymbol{\epsilon} \tag{45}$$

and consequently $\boldsymbol{t}_\epsilon = \epsilon_N\, \boldsymbol{n} + \boldsymbol{\epsilon}_T$. Hereby, $\boldsymbol{N}$ and $\boldsymbol{T}$ denote the second and third order projection tensor

$$\boldsymbol{N} = \boldsymbol{n} \otimes \boldsymbol{n} \qquad \boldsymbol{T} = \boldsymbol{n} \cdot \boldsymbol{\mathcal{I}}^{sym} - \boldsymbol{n} \otimes \boldsymbol{n} \otimes \boldsymbol{n} \tag{46}$$

and the related analytical integration of their corresponding fourth order products yields the following results

$$\begin{aligned} \tfrac{3}{4\pi}\textstyle\int_\Omega \; \boldsymbol{N} \otimes \boldsymbol{N} \; d\Omega &= \boldsymbol{\mathcal{I}}^{vol} + \tfrac{2}{5}\boldsymbol{\mathcal{I}}^{dev} \\ \tfrac{3}{4\pi}\textstyle\int_\Omega \; \boldsymbol{T}^T \cdot \boldsymbol{T} \; d\Omega &= \tfrac{3}{5}\boldsymbol{\mathcal{I}}^{dev} \; . \end{aligned} \tag{47}$$

Correspondingly, the free energy function on the microplane is introduced exclusively in terms of the two strain components and the related elastic microplane moduli $\mathcal{E}_N$ and $\mathcal{E}_T$

$$\Psi^{mic} = \frac{1}{2}\,\epsilon_N\,\mathcal{E}_N\,\epsilon_N + \frac{1}{2}\,\boldsymbol{\epsilon}_T \cdot \mathcal{E}_T\,\boldsymbol{\epsilon}_T. \tag{48}$$

The normal and tangential stress component σ_N and $\boldsymbol{\sigma}_T$ can be introduced as energetically conjugate quantities to the corresponding strains with

$$\sigma_N := \mathcal{E}_N \, \epsilon_N \qquad \boldsymbol{\sigma}_T := \mathcal{E}_T \, \boldsymbol{\epsilon}_T \tag{49}$$

and the related stress vector $\boldsymbol{t}_\sigma$ on the microplane can be expressed as $\boldsymbol{t}_\sigma = \sigma_N \, \boldsymbol{n} + \boldsymbol{\sigma}_T$. Note, however, that σ_N is not necessarily identical to the normal stresses of the previous model defined through the sum of the volumetric and the deviatoric components σ_V and σ_D as $\sigma_N \neq \sigma_V + \sigma_D$. The two–component analogue to the overall stress definition given in equation (42) can thus be expressed as

$$\boldsymbol{\sigma} = \frac{3}{4\pi} \int_\Omega \boldsymbol{N} \, \mathcal{E}_N \, \epsilon_N + \boldsymbol{T}^T \cdot \mathcal{E}_T \, \boldsymbol{\epsilon}_T \, d\Omega. \tag{50}$$

while the elastic material operator of the two–component model can be expressed in analogy to equation (43)

$$\boldsymbol{\mathcal{E}} = \frac{3}{4\pi} \int_\Omega \mathcal{E}_N \, \boldsymbol{N} \otimes \boldsymbol{N} + \mathcal{E}_T \, \boldsymbol{T}^T \cdot \boldsymbol{T} \, d\Omega. \tag{51}$$

With the help of the integration formulae (47) and the assumption of an isotropic distribution of the microplane elasticity moduli, a comparison of the coefficients of the elasticity tensor (51) with the elasticity tensor of HOOKE's law yields a relation between the microscopic elasticity moduli $\mathcal{E}_N$ and $\mathcal{E}_T$ and the macroscopic bulk and shear modulus K and G as

$$\mathcal{E}_N = 3 \, K \qquad \text{and} \qquad \mathcal{E}_T = \frac{10}{3} \, G - 2 \, K. \tag{52}$$

Remarks on the normal–tangential models

- Note, that for this class of models, the relation between the two elastic constants and the two elastic microplane moduli $\mathcal{E}_N$ and $\mathcal{E}_T$ is unique, as shown in equation (52). However, it should be mentioned, that the elastic tangential behavior is somehow related to the bulk modulus K, which is not what one intuitively expects.
- The range of validity of this class of microplane models is physically limited to positive elastic microplane moduli, such that $\mathcal{E}_N \geq 0$ and $\mathcal{E}_T \geq 0$. According to equation (52), the model is thus restricted to materials for which $G \geq \frac{3}{5} K$ which corresponds to an artificial limitation of POISSON's ratio to a range of $-1 \leq \nu \leq 0.25$.
- For this class of microplane models, the overall stress $\boldsymbol{\sigma}$ can be expressed as the integral of the symmetric part of the dyadic product of the stress vector $\boldsymbol{t}_\sigma$ with the plane's normal $\boldsymbol{n}$. Consequently, the macroscopic stress definition (50) can alternatively be expressed as $\boldsymbol{\sigma} = \frac{3}{4\pi} \int_\Omega [\boldsymbol{t}_\sigma \otimes \boldsymbol{n}]^{sym} d\Omega$. The class of microplane models introduced by JIRÁSEK [14], which have been derived in a different context, can thus be understood as a subclass of these models. Moreover, this model is identical to the microplane models without volumetric–deviatoric split as discussed by CAROL & BAŽANT [8].
- The microplane model with normal and tangential components represents the most natural microplane formulation. Since this is the type of model one would intuitively think of, its equations show a remarkable similarity with the well–known rotating and fixed crack models as shown by DE BORST, GEERS, KUHL & PEERLINGS [7] and with discrete particle models as discussed by KUHL, D'ADDETTA, HERRMANN & RAMM [17].

3.3 Comparison

A comparison of the two different classes of microplane models is shown in table 3. It documents, that the model with only one normal component as introduced in section 3.2 shows several disadvantages. Therefore, the following discussions will be restricted on the first type of microplane formulations, which are based on a volumetric deviatoric split of the normal component, as introduced in section 2.1 and specified in section 3.1.

	volumetric–deviatoric–tangential	normal–tangential
elastic constants	non–unique $\mathcal{E}_V = 3K$ $\mathcal{E}_D + \mathcal{E}_T = 10/3\,G$	uniquely determined $\mathcal{E}_N = 3K$ $\mathcal{E}_T = 10/3\,G - 2K$
coupling	fully decoupled $\mathcal{E}_V$ volumetric $\mathcal{E}_D, \mathcal{E}_T$ deviatoric	artificially coupled $\mathcal{E}_N$ volumetric $\mathcal{E}_T$ volumetric & deviatoric
range of validity	POISSON's ratio unlimited $-1 \leq \nu \leq 0.5$	POISSON's ratio limited $-1 \leq \nu \leq 0.25$
overall stresses	different from original models compare [2], [6], [11] $\boldsymbol{\sigma} \neq \frac{3}{4\pi}\int [\boldsymbol{t}_\sigma \otimes \boldsymbol{n}]^{sym} d\Omega$	similar to previous models compare [8] $\boldsymbol{\sigma} = \frac{3}{4\pi}\int [\boldsymbol{t}_\sigma \otimes \boldsymbol{n}]^{sym} d\Omega$
closely related	to discrete models	to macroscopic models

Table 3: Comparison of normal–tangential with volumetric–deviatoric–tangential models

4 Microplane damage: Choice of damage loading functions

In the context of the kinematic constraint, the microplane theory has almost exclusively been applied to elasto–damaging materials, compare BAŽANT & GAMBAROVA [2], BAŽANT & PRAT [6] and CAROL, PRAT & BAŽANT [11] for example. In this section, we will therefore reduce the generalized microplane formulation of section 2.1 to a microplane–based continuum damage model, for which the dissipative influence of plastic deformation is negligibly small. In accordance with the previous section on microplane elasticity, we will first demonstrate, how a microplane damage formulation can be extracted from the equations presented in section 2.1. The resulting formulation will thus be based on the introduction of only one damage variable d for each microplane which is governed by a single damage loading function Φ^d. In the second part of this section, however, we will discuss an alternative damage model, for which three independent damage variables d_V, d_D and d_T are introduced taking into account an independent degradation of the volumetric, the deviatoric and the tangential stiffness. Most existing microplane formulations belong to this class of models, for which three independent damage loading functions Φ^d_V, Φ^d_D and Φ^d_T have to be introduced. Finally, the two different strategies will be compared and discussed with special focus on the efficiency and numerical stability of the related algorithmic realization.

4.1 Single loading function model

The first microplane damage model is characterized through only one damage variable d introducing an equivalent degradation of the volumetric, the deviatoric and the tangential microplane stiffness. The related free energy

$$\Psi^{mic} = [1-d]\left[\frac{1}{2}\,\epsilon_V\,\mathcal{E}_V\,\epsilon_V + \frac{1}{2}\,\epsilon_D\,\mathcal{E}_D\,\epsilon_D + \frac{1}{2}\,\boldsymbol{\epsilon}_T\cdot\boldsymbol{\mathcal{E}}_T\,\boldsymbol{\epsilon}_T\right] \tag{53}$$

defines the corresponding nominal stresses

$$\sigma_V := [1-d]\,\mathcal{E}_V\epsilon_V \qquad \sigma_D := [1-d]\,\mathcal{E}_D\epsilon_D \qquad \boldsymbol{\sigma}_T := [1-d]\,\boldsymbol{\mathcal{E}}_T\boldsymbol{\epsilon}_T \tag{54}$$

and the driving force for the damage evolution

$$Y := \frac{1}{2}\,\epsilon_V\,\mathcal{E}_V\,\epsilon_V + \frac{1}{2}\,\epsilon_D\,\mathcal{E}_D\,\epsilon_D + \frac{1}{2}\,\boldsymbol{\epsilon}_T\cdot\boldsymbol{\mathcal{E}}_T\,\boldsymbol{\epsilon}_T. \tag{55}$$

Thus, the elastic domain is bounded by a single damage loading function Φ^d

$$\Phi^d = \phi^d(Y) - d(\kappa^d) \tag{56}$$

which induces a volumetric–deviatoric coupling in the inelastic regime. The corresponding KUHN–TUCKER conditions and the consistency condition

$$\Phi^d \le 0 \qquad \dot{\kappa}^d \ge 0 \qquad \Phi^d\,\dot{\kappa}^d = 0 \qquad \dot{\Phi}^d\,\dot{\kappa}^d = 0 \tag{57}$$

define the loading–unloading conditions. The consistency condition yields the equivalence $\dot{Y} = \dot{\gamma}^d$ which allows for an explicit update formula for the damage variable, as

$$d = \phi^d(\kappa^d) \qquad \text{with} \qquad \kappa^d = \max_{-\infty<t<\tau}(Y(t), \kappa_0^d). \tag{58}$$

Consequently, the overall stress tensor

$$\boldsymbol{\sigma} = \frac{3}{4\pi}\int_\Omega [1-d]\left[\mathcal{E}_V\,\boldsymbol{V}\otimes\boldsymbol{V} + \mathcal{E}_D\,\boldsymbol{D}\otimes\boldsymbol{D} + \boldsymbol{\mathcal{E}}_T\boldsymbol{T}^T\cdot\boldsymbol{T}\right] d\Omega : \boldsymbol{\epsilon} \tag{59}$$

and the tangent operator take the following form

$$\begin{aligned}\boldsymbol{\mathcal{E}}^{ed}_{tan} = \frac{3}{4\pi}\int_\Omega & [1-d]\left[\mathcal{E}_V\boldsymbol{V}\otimes\boldsymbol{V} + \mathcal{E}_D\boldsymbol{D}\otimes\boldsymbol{D} + \boldsymbol{\mathcal{E}}_T\boldsymbol{T}^T\cdot\boldsymbol{T}\right] \quad d\Omega \\ - \frac{3}{4\pi}\int_\Omega & \frac{\partial\phi^d}{\partial\kappa^d}\,\frac{\left[\boldsymbol{V}\sigma_V + \boldsymbol{D}\sigma_D + \boldsymbol{T}^T\cdot\boldsymbol{\sigma}_T\right]}{1-d}\otimes\frac{\left[\sigma_V\boldsymbol{V} + \sigma_D\boldsymbol{D} + \boldsymbol{\sigma}_T\cdot\boldsymbol{T}\right]}{1-d}\,d\Omega.\end{aligned} \tag{60}$$

Remarks on the one damage parameter model

- The structure of the overall tangent operator (60) indicates, that a volumetric–deviatoric coupling has been introduced through the damage loading function manifesting itself in the second integral expression. This coupling is an essential feature to model the pressure–sensitive behavior of cohesive frictional materials.
- In the numerical computation, the model requires the relatively low storage of one history parameter κ for each microplane.
- Numerical calculations have shown, that the choice of only one loading function leads to a computationally stable and robust numerical calculation procedure.

4.2 Multiple loading function model

In the original microplane formulation, the damage behavior is controlled separately for each component. Consequently, three individual damage variables d_V, d_D and d_T have to be introduced and the free energy can be expressed in the following form

$$\Psi^{mic} = [1-d_V]\,\frac{1}{2}\,\epsilon_V\,\mathcal{E}_V\,\epsilon_V + [1-d_D]\,\frac{1}{2}\,\epsilon_D\,\mathcal{E}_D\,\epsilon_D + [1-d_T]\,\frac{1}{2}\,\boldsymbol{\epsilon}_T\cdot\boldsymbol{\mathcal{E}}_T\,\boldsymbol{\epsilon}_T. \tag{61}$$

It defines the microplane stresses

$$\sigma_V := [1-d_V]\,\mathcal{E}_V\epsilon_V \qquad \sigma_D := [1-d_D]\,\mathcal{E}_D\epsilon_D \qquad \boldsymbol{\sigma}_T := [1-d_T]\,\boldsymbol{\mathcal{E}}_T\boldsymbol{\epsilon}_T \tag{62}$$

and the three conjugate quantities to the damage variables as

$$Y_V := \frac{1}{2}\,\epsilon_V\,\mathcal{E}_V\,\epsilon_V \qquad Y_D := \frac{1}{2}\,\epsilon_D\,\mathcal{E}_D\,\epsilon_D \qquad Y_T := \frac{1}{2}\,\boldsymbol{\epsilon}_T\cdot\boldsymbol{\mathcal{E}}_T\,\boldsymbol{\epsilon}_T. \tag{63}$$

Furthermore, three different damage loading functions

$$\Phi_V^d = \phi_V^d(Y_V) - d_V(\kappa_V^d) \qquad \Phi_D^d = \phi_D^d(Y_D) - d_D(\kappa_D^d) \qquad \Phi_T^d = \phi_T^d(Y_T) - d_T(\kappa_T^d) \tag{64}$$

have to be introduced. The loading process is thus governed by the three sets of KUHN–TUCKER loading–unloading conditions and the related consistency conditions

$$\begin{array}{llll}
\Phi_V^d \le 0 & \dot\kappa_V^d \ge 0 & \Phi_V^d\,\dot\kappa_V^d = 0 & \dot\Phi_V^d\,\dot\kappa_V^d = 0 \\
\Phi_D^d \le 0 & \dot\kappa_D^d \ge 0 & \Phi_D^d\,\dot\kappa_D^d = 0 & \dot\Phi_D^d\,\dot\kappa_D^d = 0 \\
\Phi_T^d \le 0 & \dot\kappa_T^d \ge 0 & \Phi_T^d\,\dot\kappa_T^d = 0 & \dot\Phi_T^d\,\dot\kappa_T^d = 0,
\end{array} \tag{65}$$

which can be evaluated independently yielding the following update formulae for the damage variables

$$d_V = \phi_V^d(\kappa_V^d) \qquad d_D = \phi_D^d(\kappa_D^d) \qquad d_T = \phi_T^d(\kappa_T^d), \tag{66}$$

whereby the three history parameters κ_V^d, κ_D^d and κ_T^d are defined as follows

$$\kappa_V^d = \max_{-\infty<t<\tau}(Y_V(t), \kappa_{V\,0}^d) \qquad \kappa_D^d = \max_{-\infty<t<\tau}(Y_D(t), \kappa_{D\,0}^d) \qquad \kappa_T^d = \max_{-\infty<t<\tau}(Y_T(t), \kappa_{T\,0}^d). \tag{67}$$

Consequently, the overall stress tensor $\boldsymbol{\sigma}$

$$\boldsymbol{\sigma} = \frac{3}{4\pi}\int_\Omega [1-d_V]\mathcal{E}_V\,\boldsymbol{V}\otimes\boldsymbol{V} + [1-d_D]\mathcal{E}_D\,\boldsymbol{D}\otimes\boldsymbol{D} + \boldsymbol{T}^T\cdot[1-d_T]\boldsymbol{\mathcal{E}}_T\cdot\boldsymbol{T}d\Omega : \boldsymbol{\epsilon} \tag{68}$$

and the overall tangent operator $\boldsymbol{\mathcal{E}}_{tan}^{ed}$ can be expressed in the following form

$$\begin{aligned}
\boldsymbol{\mathcal{E}}_{tan}^{ed} = {} & \frac{3}{4\pi}\int_\Omega [1-d_V]\mathcal{E}_V\;\boldsymbol{V}\otimes\boldsymbol{V} + [1-d_D]\mathcal{E}_D\;\boldsymbol{D}\otimes\boldsymbol{D} + \boldsymbol{T}^T\cdot[1-d_T]\boldsymbol{\mathcal{E}}_T\cdot\boldsymbol{T}\,d\Omega \\
& - \frac{3}{4\pi}\int_\Omega \frac{\partial\phi_V^d}{\partial\kappa_V^d}\frac{\sigma_V^2}{[1-d_V]^2}\,\boldsymbol{V}\otimes\boldsymbol{V} + \frac{\partial\phi_D^d}{\partial\kappa_D^d}\frac{\sigma_D^2}{[1-d_D]^2}\,\boldsymbol{D}\otimes\boldsymbol{D} + \boldsymbol{T}^T\cdot\frac{\partial\phi_T^d}{\partial\kappa_T^d}\frac{\boldsymbol{\sigma}_T\otimes\boldsymbol{\sigma}_T}{[1-d_T]^2}\cdot\boldsymbol{T}\,d\Omega.
\end{aligned} \tag{69}$$

Remarks on the three damage parameter model

- The structure of the tangent operator (69) documents, that due to the introduction of three individual damage variables, the volumetric, the deviatoric and the tangential component remain decoupled even in the inelastic regime. From a physical point of view, this assumption does not seem reasonable especially when modelling pressure–sensitive materials. It has been shown, that models based on a complete decoupling are unable to simulate the behavior of cohesive frictional materials such as concrete, compare for example BAŽANT & PLANAS [5] or OŽBOLT & BAŽANT [22].
- Since the volumetric material response is only influenced by the volumetric strain state, it is identical for each microplane. The volumetric response can thus be calculated globally independent from the deviatoric material behavior.
- From a computational point of view, the model with three damage variables requires a relatively high storage. In addition to the global volumetric history parameter κ_V, a deviatoric and a tangential history parameter κ_D and κ_T need to be stored for each microplane, compare CAROL & BAŽANT [8].
- During numerically simulated loading processes, an artificial unloading–reloading has been observed especially for the deviatoric and the tangential component. This instability seems to be caused by the fact, that both components affect the deviatoric material behavior.

4.3 Comparison

	one loading function	three loading functions
degradation	all components identical d one single variable	each component individually d_V, d_D, d_T three variables
coupling	inelastically coupled $\Phi^d = \Phi^d(\epsilon_V, \epsilon_D, \epsilon_T)$	fully decoupled $\Phi^d_V = \Phi^d_V(\epsilon_V)$ $\Phi^d_D = \Phi^d_D(\epsilon_D)$ $\Phi^d_T = \Phi^d_T(\epsilon_T)$
storage	acceptable κ^d for each microplane	relatively large κ^d_V globally κ^d_D, κ^d_T for each microplane
application	all materials including pressure–sensitive materials	restricted to pressure–insensitive materials

Table 6: Comparison of models with single loading function and multiple loading functions

It has been shown, that the second class of models which is based on the introduction of several independent loading functions is more expensive from a computational point of view. It requires the storage of a large number of internal variables. However, it is unable to characterize the behavior of pressure–sensitive materials and moreover may even lead to computational instabilities. For these reasons, the first class of models, which

enables a controlled volumetric–deviatoric coupling in the inelastic regime is considered more attractive. Note, however, that with this model, the volumetric, the deviatoric and the tangential stiffness exhibit an equivalent amount of degradation. The above remarks are once again summarized table 6.

5 Microplane plasticity: Choice of microplane parameters

In this section, it will be demonstrated, how the inelastic microplane parameters can be related to macroscopically measurable quantities. Therefore, the constitutive equations presented in section 2.1 will be reduced to microplane plasticity, by setting $d \equiv 0$. In the first part of this section, a microplane plasticity formulation based on a DRUCKER–PRAGER yield function will be discussed, compare IORDACHE & WILLAM [13] for a detailed interpretation. In the second part, a similar plasticity formulation will be introduced in terms of the invariants of the overall stress tensor. A comparison of the corresponding coefficients enables the characterization of the microscopic friction coefficient and the microscopic yield stress in terms of the uniaxial tensile and compressive strength. For the sake of simplicity, we will assume, that in the following model, the deviatoric elasticity modulus vanishes identically as $\mathcal{E}_D \equiv 0$. According to equation (44), the remaining microplane elasticity moduli take the values $\mathcal{E}_V = 3\,K$ and $\mathcal{E}_T = 10\,/\,3\,G$.

5.1 Microplane–based Drucker–Prager plasticity

The model is thus based on only two strain components, a volumetric and a deviatoric one,

$$\epsilon_V = \boldsymbol{V} : \boldsymbol{\epsilon} = \epsilon_V^e + \epsilon_V^p \qquad \boldsymbol{\epsilon}_T = \boldsymbol{T} : \boldsymbol{\epsilon} = \boldsymbol{\epsilon}_T^e + \boldsymbol{\epsilon}_T^p \tag{70}$$

which can be additively decomposed into elastic and plastic parts. The free energy

$$\Psi^{mic} = \frac{1}{2}[\epsilon_V - \epsilon_V^p]\,\mathcal{E}_V\,[\epsilon_V - \epsilon_V^p] + \frac{1}{2}[\boldsymbol{\epsilon}_T - \boldsymbol{\epsilon}_T^p]\cdot\mathcal{E}_T\,[\boldsymbol{\epsilon}_T - \boldsymbol{\epsilon}_T^p] + \int_0^{\kappa^p} \phi^{pmic}\,d\hat{\kappa} \tag{71}$$

defines the microplane stresses conjugate to the elastic microplane strains

$$\begin{aligned} \sigma_V &:= \frac{\partial \Psi^{mic}}{\partial \epsilon_V} & \dot{\sigma}_V &= \mathcal{E}_V\,[\dot{\epsilon}_V - \dot{\epsilon}_V^p] \\ \boldsymbol{\sigma}_T &:= \frac{\partial \Psi^{mic}}{\partial \boldsymbol{\epsilon}_T} & \dot{\boldsymbol{\sigma}}_T &= \mathcal{E}_T\,[\dot{\boldsymbol{\epsilon}}_T - \dot{\boldsymbol{\epsilon}}_T^p]. \end{aligned} \tag{72}$$

In accordance with the classical macroscopic yield function of the DRUCKER–PRAGER type; the yield function on the microplane as introduced in (13) is specified in the following form

$$\Phi^{pmic} = \frac{1}{\sqrt{2}}\,||\boldsymbol{\sigma}_T|| + \alpha^{pmic}\sigma_V - \phi^{pmic}. \tag{73}$$

whereby, $||(\bullet)|| = \sqrt{(\bullet)^2}$. Note, that due to the introduction of only one yield function, a volumetric deviatoric coupling, which is controlled through the friction coefficient α^{pmic}, is taken into account. With the help of the flow rule (16), the KUHN–TUCKER conditions

(17) and the equation for the plastic multiplier (18) the evolution of the overall stress tensor can be expressed as a special case of (20) as

$$\dot{\boldsymbol{\sigma}} = \frac{3}{4\pi} \int_{\Omega} V \mathcal{E}_V [\dot{\epsilon}_V - \dot{\epsilon}_V^p] + \boldsymbol{T}^T \cdot \boldsymbol{\mathcal{E}}_T [\dot{\boldsymbol{\epsilon}}_T - \dot{\boldsymbol{\epsilon}}_T^p] \, d\Omega. \tag{74}$$

Moreover, the overall tangent operator $\boldsymbol{\mathcal{E}}_{tan}^{ep}$ can be extracted from its general form (22)

$$\begin{aligned} \boldsymbol{\mathcal{E}}_{tan}^{ep} = & \frac{3}{4\pi} \int_{\Omega} \mathcal{E}_V \, \boldsymbol{V} \otimes \boldsymbol{V} + \mathcal{E}_T \, \boldsymbol{T}^T \cdot \boldsymbol{T} \quad d\Omega \\ & - \frac{3}{4\pi} \int_{\Omega} \frac{1}{h^p} \left[\boldsymbol{V} \, \mathcal{E}_V \, \mu_V + \boldsymbol{T}^T \cdot \boldsymbol{\mathcal{E}}_T \, \boldsymbol{\mu}_T \right] \otimes \left[\nu_V \, \mathcal{E}_V \, \boldsymbol{V} + \boldsymbol{\nu}_T \cdot \boldsymbol{\mathcal{E}}_T \, \boldsymbol{T} \right] d\Omega, \end{aligned} \tag{75}$$

whereby the definitions of the normals ν_V, $\boldsymbol{\nu}_T$, μ_V and $\boldsymbol{\mu}_T$ have been given in equations (14) and (15).

5.2 Classical invariant–based Drucker–Prager plasticity

In contrast to the microscopic yield function (73) the classical macroscopic DRUCKER–PRAGER yield function

$$\Phi^{p\,mac} = \sqrt{J_2} + \alpha^{p\,mac} I_1 - \phi^{p\,mac} \tag{76}$$

is based on the first invariant of the stress tensor I_1 and the second invariant of its deviator J_2. It is governed by two parameters, namely the macroscopic friction coefficient $\alpha^{p\,mac}$ and the macroscopic yield stress $\phi^{p\,mac}$, which can be identified uniquely through a uniaxial tension and compression test. Before the onset of plastic yielding, in the elastic regime, the invariants of the overall stress tensor $\boldsymbol{\sigma}$ can directly be related to the microplane stress components σ_V and $\boldsymbol{\sigma}_T$ as

$$\begin{aligned} I_1 &= \quad \boldsymbol{\sigma} : \boldsymbol{1} \quad = \frac{3}{4\pi} \int_{\Omega} \quad \sigma_V \quad d\Omega \\ J_2 &= \frac{1}{2} \boldsymbol{\sigma}^{dev} : \boldsymbol{\sigma}^{dev} = \frac{3}{4\pi} \int_{\Omega} \frac{3}{10} \boldsymbol{\sigma}_T \cdot \boldsymbol{\sigma}_T \, d\Omega. \end{aligned} \tag{77}$$

If the material behaves elastically, we can assume that the macroscopic DRUCKER–PRAGER yield function (76) can be expressed as the integral of all microplane yield functions over the solid angle Ω

$$\Phi^{p\,mac} \approx \frac{3}{4\pi} \int_{\Omega} \Phi^{p\,mic} \, d\Omega. \tag{78}$$

Note, that this assumption is only valid in the elastic regime and in a final state, in which all microplanes have entered the plastic regime. In general, we cannot expect all microplanes to start yielding simultaneously. Thus, a transition zone between these two stages can be observed, which is characterized through a progressive onset of yielding such that more and more microplanes enter the plastic state. However, if we consider equation (78) as an approximation, it can help to understand how to determine the values of the microplane parameters $\alpha^{p\,mic}$ and $\phi^{p\,mic}$. Therefore, the following integration formulae according to KUHL, RAMM & WILLAM [19] have to be applied

$$\begin{aligned} \frac{3}{4\pi} \int_{\Omega} \frac{1}{\sqrt{2}} \|\boldsymbol{\sigma}_T\| \, d\Omega &= \sqrt{\frac{5}{3}} \sqrt{J_2} \\ \frac{3}{4\pi} \int_{\Omega} \alpha^{p\,mic} \sigma_V \, d\Omega &= \alpha^{p\,mic} \quad I_1 \\ \frac{3}{4\pi} \int_{\Omega} \quad \phi^{p\,mic} \quad d\Omega &= \phi^{p\,mic} \quad 3 \quad . \end{aligned} \tag{79}$$

Finally, a comparison of the coefficients of the macroscopic yield function (76) and the integral over all microscopic yield functions (73)

$$\begin{aligned} \Phi^{p\,mac} &= \sqrt{J_2} + \alpha^{p\,mac}\, I_1 - \phi^{p\,mac} \\ \frac{3}{4\pi}\int_\Omega \Phi^{p\,mic}\, d\Omega &= \sqrt{\frac{5}{3}}\sqrt{J_2} + \alpha^{p\,mic}\, I_1 - 3\,\phi^{p\,mic} \end{aligned} \tag{80}$$

yields the following relations between the microscopic and the microscopic friction coefficients and yield stresses

$$\alpha^{p\,mic} \approx \sqrt{\frac{5}{3}}\,\alpha^{p\,mac} \qquad \text{and} \qquad \phi^{p\,mic} \approx \frac{\sqrt{5}}{3\sqrt{3}}\,\phi^{p\,mac}. \tag{81}$$

The macroscopic DRUCKER–PRAGER parameters can be determined from a uniaxial tension and compression test and can thus be expressed in terms of the uniaxial tensile and compressive strength f_t and f_c. Consequently, the microplane parameters can be expressed in terms of macroscopically measurable quantities as

$$\begin{aligned} \alpha^{p\,mac} &= \frac{1}{\sqrt{3}}\,\frac{f_c - f_t}{f_c + f_t} \qquad \text{and} \qquad \phi^{p\,mac} = \frac{2}{\sqrt{3}}\,\frac{f_c\, f_t}{f_c + f_t} \\ \alpha^{p\,mic} &\approx \frac{\sqrt{5}}{3}\,\frac{f_c - f_t}{f_c + f_t} \qquad \text{and} \qquad \phi^{p\,mic} \approx \frac{2\sqrt{5}}{9}\,\frac{f_c\, f_t}{f_c + f_t}. \end{aligned} \tag{82}$$

5.3 Comparison – Plate with a hole

Finally, the microplane–based plasticity formulation and the invariant–based macroscopic plasticity model will be compared by means of the model problem of a plate with a hole, compare BARTHOLD, SCHMIDT & STEIN [1]. Originally, the presented model was developed for cohesive frictional materials. However, in this example, a classical pressure–insensitive metallic material, aluminium, has been chosen. The aluminum plate, for which a plane strain state is assumed, has a size of 200 × 200 mm^2, while the radius of the hole is r = 10 mm. The plate is loaded vertically under displacement control with $\lambda\,\bar{p}$, whereby $\bar{p}$ = 100 MPa. The material is characterized through a Young's modulus of E = 206900 N/mm^2 and a Poisson's ratio of $\nu = 0.29$, such that $\mathcal{E}_V$ = 492619.05 N/mm^2, $\mathcal{E}_D$ = 0 N/mm^2 and $\mathcal{E}_T$ = 267312.66 N/mm^2. Moreover, a perfectly plastic material behavior is assumed with $f_c = f_t$ = 450 N/mm^2. Consequently, the microscopic and the macroscopic friction coefficient vanish identically as $\alpha^{p\,mac} = 0$ and $\alpha^{p\,mic} = 0$, while the macroscopic and the microplane–based yield strength take values of $\phi^{p\,mac}$ = 259.81 N/mm^2 and $\phi^{p\,mic}$ = 111.80 N/mm^2. For the spatial discretization, 256 eight–noded finite elements with a reduced 2 × 2 integration have been applied. Moreover, the spatial discretization of the solid angle has been performed with $n_{mp} = 42$ integration points as proposed by BAŽANT & OH [3]. Figure 5 depicts the resulting load–deflection curves of both simulations. The critical load factor of the macroscopic model $\lambda^{mac}_{crit} = 4.66$ corresponds to the reference solution given by BARTHOLD, SCHMIDT & STEIN [1]. Remarkably, the critical load factor of the microplane plasticity model $\lambda^{mic}_{crit} = 4.30$ is slightly lower. This difference is caused by the fact, that on several microplanes, the yield condition is violated before the yield stress is reached macroscopically. Then, a successive onset of yielding can be observed on more and more microplanes until all planes of the corresponding integration point have finally entered the plastic regime. Despite this slight difference, both models behave rather similarly. The related strain distributions at a top displacement of $u = 0.0025$ mm shown in figure

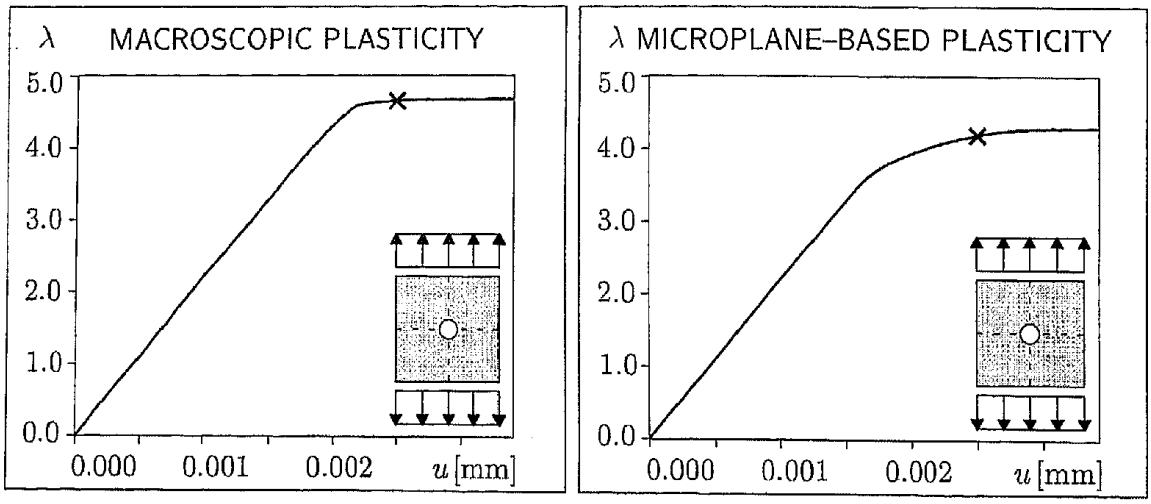

Figure 5: Macroscopic and microscopic model – Load displacement curves

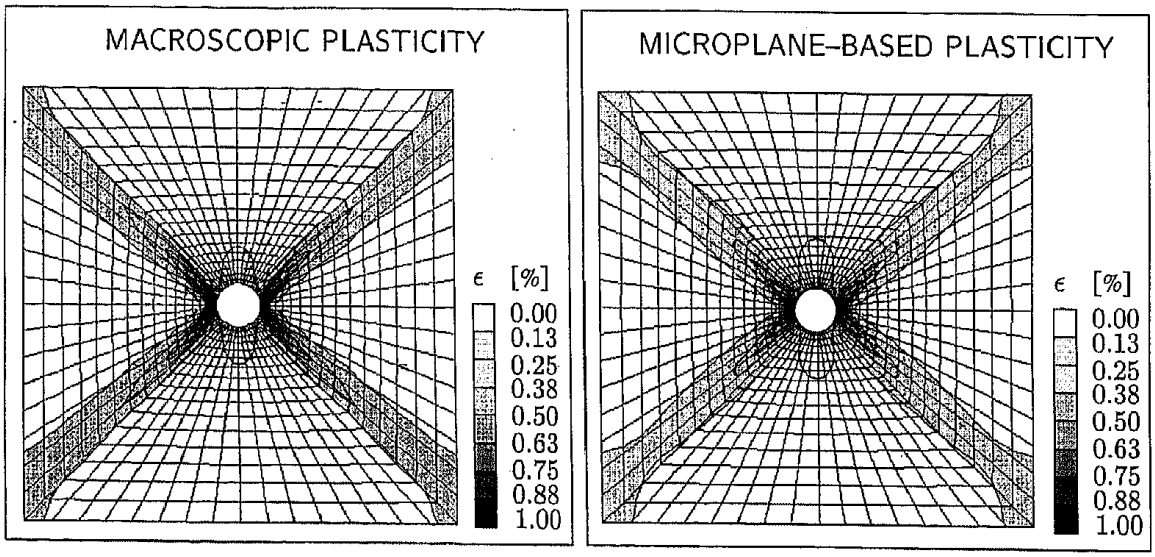

Figure 6: Macroscopic and microscopic model – Strains in loading direction

6 underline the similarity of the different formulations. In both cases, plastic yielding is initiated at the horizontal edges of the hole and a zone of localized deformation forms under an angle of 45^0 towards the loading axis. It should be mentioned, that for the sake of simplicity, this comparison has only been shown for a rather simple material formulation, but more complex studies involving pressure–sensitive materials are straightforward.

6 Conclusion

In this paper, different aspects of microplane modelling have been highlighted. The basic idea of the microplane concept has been introduced for microplane elasto–plasticity coupled to microplane damage. Thereby, the assumption of a kinematic constraint defined three strain components for each microplane. A related plastic yield surface and a damage loading function were introduced to define the elastic domain on the microplane level. In a second step, an alternative microplane formulation based on only two components

has been discussed in the context of microplane elasticity. Its obvious disadvantage is an artificial coupling of the normal and the tangential behavior through the bulk modulus. Another alternative strategy based on the introduction of independent loading functions for each microplane component has been illustrated in the context of microplane damage. However, the introduction of individual loading functions requires the storage of a larger number of internal variables. Moreover, it results in a fully decoupled volumetric deviatoric material characterization which is non–physical for most non–metallic materials. Consequently, the three component model with a single damage and plastic yield function is considered to be a better choice.
As a typical representative of this class, microplane plasticity has been analyzed. Special focus was dedicated to the choice of the related microplane parameters, which can be expressed in terms of macroscopically measurable quantities in several specific cases. This approach has been validated by a comparison of a microplane–based DRUCKER–PRAGER plasticity formulation with the classical macroscopic DRUCKER–PRAGER model.
In summary, this paper documents the potential of the microplane concept to simulate an anisotropic material behavior which is not yet fully exploited. Due to several small modifications of the original microplane model from the literature, a controlled volumetric deviatoric coupling can be taken into account. Moreover, in contrast to the original model, the class of microplane models presented in this paper is formulated in a thermodynamically consistent fashion and can thus guarantee the satisfaction of the second principle of thermodynamics. Future work will be dedicated to the application of this basic concept to various different materials such as concrete, reinforced concrete or wood.

Acknowledgement

The present study is supported by grants of the German National Science Foundation DFG within the research project Ra 218/18. This support is gratefully acknowledged.

References

[1] BARTHOLD, F.-J., M. SCHMIDT & E. STEIN [1998]. 'Error indicators and mesh refinements for finite element computations of elastoplastic deformations.' *Comp. Mech.*, **22**, pp. 225–238.

[2] BAŽANT, Z. P. & P. G. GAMBAROVA [1984]. 'Crack shear in concrete: Crack band microplane model.' *J. Struct. Eng., ASCE*, **110**, pp. 2015–2036.

[3] BAŽANT, Z. P. & B. H. OH [1985]. 'Microplane model for progressive fracture of concrete and rock.' *J. Eng. Mech.*, **111**, pp. 559–582.

[4] BAŽANT, Z. P. & J. OŽBOLT [1992]. 'Compression failure of quasibrittle material: Nonlocal microplane model.' *J. Eng. Mech.*, **118**, pp. 540–556.

[5] BAŽANT, Z. P. & J. PLANAS [1998]. *Fracture and Size Effect in Concrete and other Quasibrittle Materials*. CRC Press.

[6] BAŽANT, Z. P. & P. PRAT [1988]. 'Microplane model for brittle plastic material: Part I – Theory, Part II – Verification.' *J. Eng. Mech.*, **114**, pp. 1672–1702.

[7] DE BORST, R., M. G. D. GEERS, E. KUHL & R. H. J. PEERLINGS [1998]. 'Enhanced damage models for concrete fracture.' In *Computational Modelling of Concrete Structures*, edited by R. de Borst, N. Bićanić, H. Mang & G. Meschke, pp. 231–248. Balkema, Rotterdam.

[8] CAROL, I. & Z. P. BAŽANT [1997]. 'Damage and plasticity in microplane theory.' *Int. J. Solids & Structures*, **34**, pp. 3807–3835.

[9] CAROL, I., Z. P. BAŽANT & P. PRAT [1991]. 'Geometric damage tensor based on microplane model.' *J. Eng. Mech.*, **117**, pp. 2429–2448.

[10] CAROL, I., M. JIRÁSEK & Z. BAŽANT [1999]. 'A thermodynamically consistent approach to microplane theory.' *Int. J. Solids & Structures, submitted for publication.*

[11] CAROL, I., P. PRAT & Z. P. BAŽANT [1992]. 'New explicit microplane model for concrete: Theoretical aspects and numerical implementation.' *Int. J. Solids & Structures*, **29**, pp. 1173–1191.

[12] FICHANT, S., C. LA BORDERIE & G. PIJAUDIER-CABOT [1999]. 'Isotropic and anisotropic descriptions of damage in concrete structures.' *Mech. Coh. Frict. Mat.*, **4**, pp. 339–359.

[13] IORDACHE, M. M. & K. J. WILLAM [1999]. 'Localized failure modes in cohesive frictional materials.' *Mech. Coh. Frict. Mat., submitted for publication.*

[14] JIRÁSEK, M. [1999]. 'Comments on microplane theory.' In *Mechanics of Quasi–Brittle Materials and Structures*, edited by G. Pijaudier-Cabot, Z. Bittnar & B. Gérard, pp. 57–77. Hermes Science Publications, Paris.

[15] JU, J. W. [1989]. 'On energy-based coupled elastoplastic damage theories: Constitutive modeling and computational aspects.' *Int. J. Solids & Structures*, **25**, pp. 803–833.

[16] KANATANI, K. I. [1984]. 'Distribution of directional data and fabric tensors.' *Int. J. Eng. Science*, **22**, pp. 149–164.

[17] KUHL, E., G. A. D'ADDETTA, H. J. HERRMANN & E. RAMM [1999]. 'A comparison of discrete granular material models with continuous microplane formulations.' *Granular Matter, in press.*

[18] KUHL, E., E. RAMM & R. DE BORST [1999]. 'An anisotropic gradient damage model for quasi–brittle materials.' *Comp. Meth. Appl. Mech. Eng., accepted for publication.*

[19] KUHL, E., E. RAMM & K. WILLAM [1999]. 'Failure analysis for elasto–plastic material models on different levels of observation.' *Int. J. Solids & Structures, accepted for publication.*

[20] LUBARDA, V. A. & D. KRAJCINOVIC [1993]. 'Damage tensors and the crack density distribution.' *Int. J. Solids & Structures*, **30**, pp. 2859–2877.

[21] MOHR, O. [1900]. 'Welche Umstände bedingen die Elastizitätsgrenze und den Bruch eines Materiales?' *Zeitschrift des Vereins Deutscher Ingenieure*, **46**, pp. 1524–1530, 1572–1577.

[22] OŽBOLT, J. & Z. P. BAŽANT [1992]. 'Microplane model for cyclic triaxial behavior concrete.' *J. Eng. Mech.*, **118**, pp. 1365–1386.

[23] SIMO, J. C. & J. W. JU [1987]. 'Strain– and stress based continuum damage models: Part I – Formulation, Part II – Computational aspects.' *Int. J. Solids & Structures*, **23**, pp. 821–869.